Electronic Supplementary Information

Experimental section

1. Plant material

Tomato (*Solanum lycopersicum* L.) plants (cultivar Momotaro, currently the most popular in Japan) were grown in a semi-open greenhouse at Ehime Research Institute of Agriculture, Forestry and Fisheries, Kumakogen-cho, Ehime, Japan. Seedlings were transplanted in May 2019. Red colour (according to the USDA colour grade[1]) tomatoes (30 fruits in total) were harvested on July 27, 2019. The average mass of each tomato was 242 ± 33 g. The dimensions were 84 ± 4 mm, 79 ± 4 mm, and 61 ± 2 mm for the major and minor axes and height, respectively. The colour of the tomatoes at the onset of harvesting was measured by a colorimeter (TES135A plus, TES Co., Taiwan). A circle (20 mm diameter) was measured under the D65 illuminant condition at a 2° observer angle. Three records were measured per fruit, one from the blossom end and two from the equator (180° between the measurements). The average of these records was used for one fruit. The hue and lightness were < 39.7° and < 50.5, and the averages of 30 fruits were 27.8 ± 7.9° and 44.4 ± 3.7, respectively. After the measurement of colour, the fruits were sent to Kyoto University using a commercial delivery service that maintained their temperature at 0–10 °C during transportation (24 h). After arrival, the tomatoes were stored in the dark at 25 ± 1 °C in an incubator (AS ONE Corp., Japan). The average relative humidity was maintained at 79 ± 5%. During storage, the fluorescence emission spectra of the tissues were measured (the tissues are described below). As a reference, the reflecting and fluorescence microscopic image and stained microscopic image of the cuticle were captured. At each sampling in the three experiments conducted, three fruits were used on each day up to day 13 at 3-day intervals.

2. Autofluorescence image

To confirm the autofluorescence of the tomato surface in a non-destructive manner, a photograph was captured under UVA illumination (**Fig. S1**). The normal coloured photograph was captured under a halogen lamp illumination. For the fluorescence image, a 365 nm UV LED (CCS Inc., Japan) with a long pass filter (50% cut at 430 nm) were placed in front of the camera. A digital camera, EOS Kiss x7 (Canon Inc., Japan), was used for imaging. Parameters of ISO 100, F-6.3, and shutter exposure of 1/25 s (colour) and 4 s (fluorescence) were set. The fraction of reflected light per excitation light (λ = 360 nm) is the product of reflectance and the long pass filter transmittance (i.e. R_{tomato} = 0.0103 and 0.0102 for before and after the storage of 13 days, respectively, and T_{filter} = 0.00257), yielding 2.6×10^{-5} during the storage.

3. Reflecting microscopic imaging

To confirm the structural scales of each tissue layer, reflecting microscopic images were obtained (**Fig. S2**). The set-up was similar with that for autofluorescence microscopic images (**Fig. 1**) except

for the halogen lamp as a light source. The fraction of reflected light per excitation light is estimated to be $R_{tomato} \times T_{filter} = 2.6 \times 10^{-5}$ during the storage as described in the above section.

4. Stained microscopic image of the cuticle

To investigate the structural scale of the cuticle, a stained microscopic image of the cuticle was captured (**Fig. 4**). The fixation of the pericarp until the preparation of the slide was based on the protocol of Isaacson *et al*.[2]

The first step was tissue fixation and embedding. A ring of pericarp with 5 mm width was separated from each tomato, and a cube of 5 × 5 × 5 mm^3 was cut out using a razor. The tissue cube was immediately transferred to an FAA fixative [10% formalin (37% formaldehyde, aqueous solution), 5% glacial acetic acid, 50% ethanol, 35% distilled water]. The volume ratio of the tissue to the fixative was 1:10. The solution was vacuum infiltrated for 15 min. The FAA was removed, replaced with a fresh fixative, and the samples were stored overnight at 4 °C. Then, they were cryoprotected using 10% or 20% sucrose in 100 mM PBS, as described by Isaacson *et al.* [2] The tissue cubes were then washed gently in OCT medium (Sakura Finetek Japan Co., Ltd.), and transferred to cryo-moulds (Sakura Finetek Japan Co., Ltd.). Two samples were added per mould and oriented such that their cuticles were perpendicular to the bottom of the mould and parallel to one another. The samples were frozen by dropping them into isopentane in a glass beaker, which was placed in liquid nitrogen, and then stored at −80 °C prior to sectioning.

The second step was cryo-sectioning. The tomato pericarp was cryo-sectioned with 5 μm thickness using a microtome HM450 with a dry ice tray unit 715400 (Thermo Fisher Scientific, USA). The section was transferred to adhesive-coated slides. Each slide was post-fixed at room temperature (23 °C) using FFA for 45 s and rinsed with distilled water prior to staining.

The third step was Oil Red O staining and microscopic observation. Oil Red O (FUJIFILM Wako Pure Chemical Corp., Japan) stock solution (0.3 w/v% in isopropanol) was diluted 6:4 with distilled water, mixed thoroughly, allowed to sit at room temperature (23 °C) for 30 min, and then filtered. The sections were stained for 30 min, as described by Martin and Rose,[3] and then rinsed first with 50% isopropanol, and then with distilled water.[4] The tissue section with 5 μm thickness stained with Oil Red O was imaged using a light microscope Motic BA 200 (Shimadzu Corp., Japan) equipped with an objective PLAN 40×/0.65.

Table S1 Tissue, cell types, and thickness.

Tissue†	Cell types‡	Thickness (μm)§	
Code	**Code**	**Range**	**Mean ± S.E.**
3-mm-thick	cu, epi cells, sub-epi cells, col cells, par cells	3×10^3	3×10^3 ± n.a.
peel	cu, epi cells, sub-epi cells, col cells	86−486	259 ± 26
epi	cu, epi cells, sub-epi cells	42−143	70 ± 4
cu	cu	26−40	32 ± 1

† Tissue codes of 3-mm-thick, epi, cu stand for 3-mm-thick sample, epidermis and cuticle, respectively.

‡ Cell type codes of cu, epi cell, sub-epi cell, col cell and par cell stand for cuticle, epidermal cell, sub-epidermal cell, collenchyma cell and parenchyma cell, respectively.

§ The thickness is the mean ± standard error of 28, 29 and 30 tomato samples for peel, epidermis and cuticle, respectively.

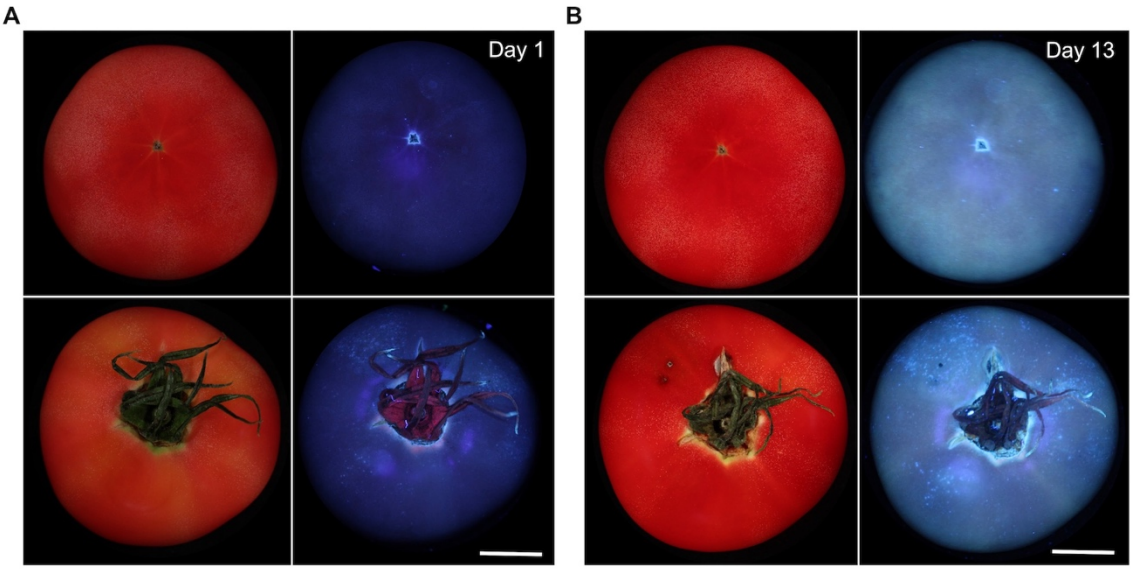

Fig. S1 Autofluorescence image of tomato at day 1 (A) and day 13 (B) after the harvest at red ripe stage and storage at 25 °C. Color image (left) and fluorescence image (right). Each image was taken separately. The excitation wavelength was 365 nm. The fluorescence image depends on the RGB sensitivity. Bar = 20 mm.

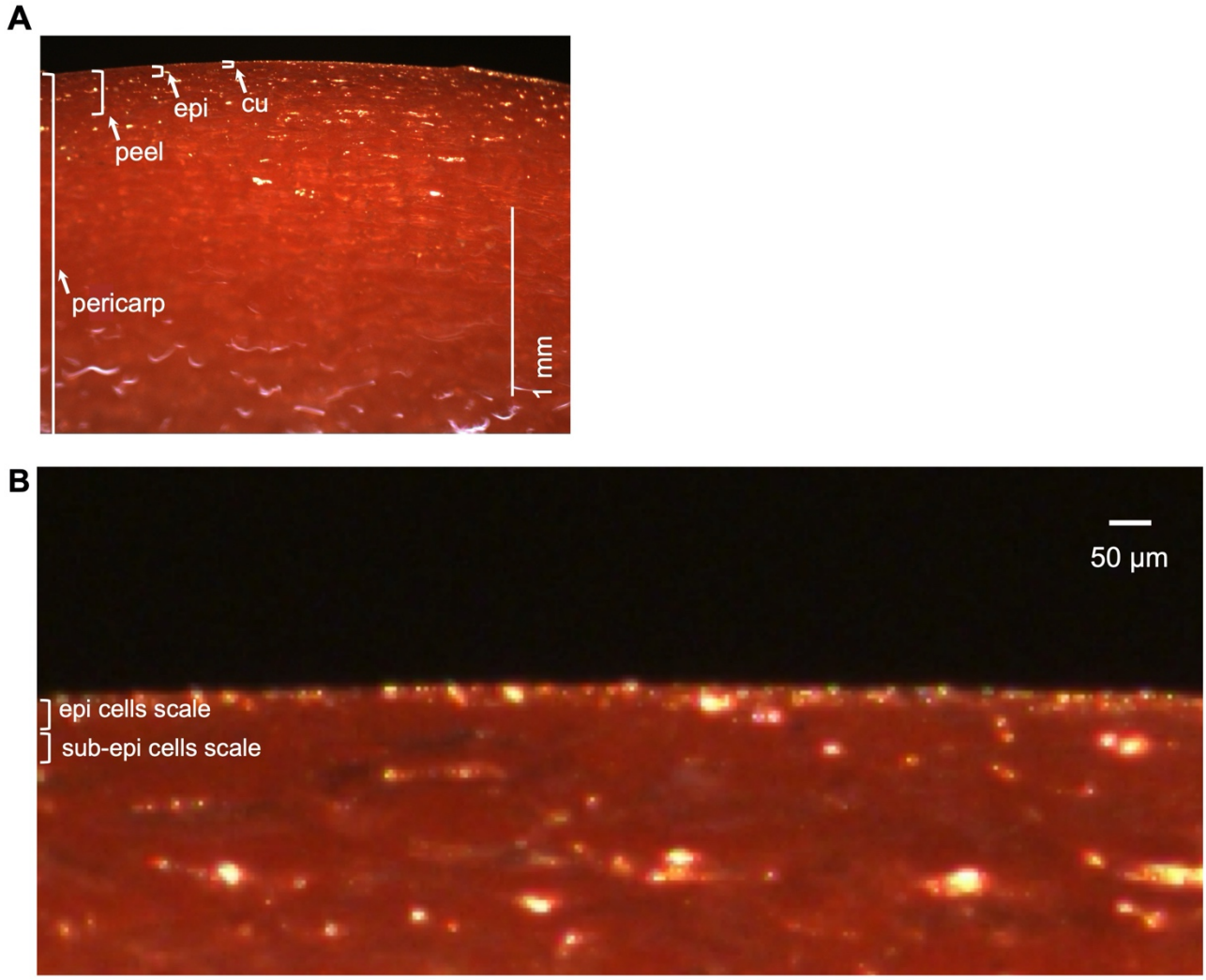

Fig. S2 Reflecting microscopic image of tomato at the harvest (A) and its magnification (B). See Table S1 for the tissue and cell type codes. The boundary of each part is approximated based on the scale (see **Table S1**).

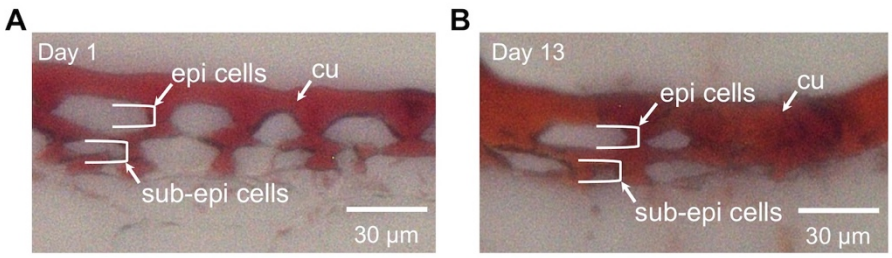

Fig. S3 (A) Oil Red O stained light microscopic image of the tomato cuticle at the harvest and (B) after storage at 25 °C until day 13. The cuticle is stained red.

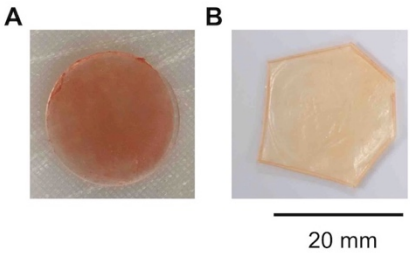

Fig. S4 Photographs of isolated tomato epidermis (A) and cuticle (B) at day 1. Bar = 20 mm.

Appendix

Experimental section

1. Calculation of apparent fluorescence quantum yield

As an appendix, we calculated the apparent fluorescence quantum yield of tomato fruits before and after the storage of 13 days. The apparent value means that this value was the obtained by assuming the several fluorophores as one, weighted by coefficient c:

$$\Phi = \sum_i c_\mathrm{i} \Phi_\mathrm{i},$$

Eq. (A1)

where Φ and Φ_i are the apparent and authentic quantum yields, respectively. c_i is the weighted coefficient for its constituents. We call this apparent quantum yield as a fluorescence quantum yield hereafter.

In diffusely reflected sample, relationship between the fluorescence quantum yields Φ, observed fluorescence emission spectra F and the effective reflectance R_eff are related with the equation[5]:

$$\Phi = q \frac{F}{R_\mathrm{eff}}$$

Eq. (A2)

where q is a proportionality constant, that can be calibrated using a standard[5]. However, in this paper, we estimate the quantum yield in a simpler way based on the modified Lambert-Beer's law[6] as follows (It is noted that the following method does not consider re-absorption contribution to the fluorescence). In microscopic interpretation of Lambert-Beer's law, a fraction of absorbed photons 1-exp(-2.303εcl) emit the fluorescence with the efficiency Φ:

$$F = (1 - \mathrm{e}^{-2.303\varepsilon cl})\Phi I_0,$$

Eq. (A3)

where ε, c, l, I_0 are the optical absorption coefficient, concentration of the fluorophore, optical path length and the incident light power, respectively. For a thin medium where $2.303\varepsilon cl \ll 1$, we can approximate the above equation as

$$F = 2.303\varepsilon cl\Phi I_0.$$

Eq. (A4)

From the Eq. (A4), the fluorescence quantum yield is calculated by

$$\Phi = \Phi_{\mathrm{st}} \cdot \frac{F}{F_{\mathrm{st}}} \cdot \frac{A_{\mathrm{st}}}{A} \cdot \frac{n^2}{{n_{\mathrm{st}}}^2},$$

Eq. (A5)

which is so called as a relative determination[7,8]. Here, Φ and Φ_{st} are the fluorescence quantum yields with a subscript of st for a standard. F and F_{st} are the fluorescence spectral area. n and n_{st} are the refractive indices at the excitation wavelength. A and A_{st} are the absorbance in the optical path, which are connected with ε, c and l with the equation:

$$A = 2.303\varepsilon cl.$$

Eq. (A6)

In our case, both the standard rhodamine B and tomato tissues consists of water since the moisture content in the peel are 80−90% in our samples, the refractive index factor was approximated as one.

$$\Phi = \Phi_{\mathrm{st}} \cdot \frac{F}{F_{\mathrm{st}}} \cdot \frac{A_{\mathrm{st}}}{A}.$$

Eq. (A7)

It is noted that this equation does not consider any re-absorption contribution to the fluorescence spectra nor Rayleigh scattering contribution to the absorbance spectra, which underestimate or overestimate the fluorescence quantum yields of tomato sample, respectively.

2. Fluorescence area and absorbance in the optical path

To estimate a fluorescence quantum yield Φ using the Eq. (1), we measured the fluorescence spectral area (F) and the absorbance (A) in the corresponding optical path for two samples: tomato samples and rhodamine B standard (**Table A1**). The rhodamine B solution was prepared by dissolving the rhodamine B powder (WAKO pure chemical Corp.) in the ethanol at the concentration of 3 g L^{-1}. Then, the solution was diluted into the final concentration of 45 and 90 μg L^{-1}, yielding 0.094 and 0.19 μM solution, respectively. The fluorescence area F was calculated by integrating the intensity under the spectral curve in the wavelength range of 390 to 700 nm (λ_{ex} = 360 nm). The spectra were measured using fluorophotometer FP-8300 (JASCO Corp.) in a right-angle geometry (90 ° detection) with a 10-mm cell (**Fig. A1**). The absorbance A in the corresponding optical path length (10 mm) was calculated using an absorption coefficient from the literature value[9].

The fluorescence spectra of tomato samples were measured before and after the storage for 13 days. The spectra were measured using the same device for the standard but in a front-face

geometry (60 ° incidence and 30 ° detection). The absorbance A in the corresponding optical path was calculated as a logarithmetic value of the reciprocal of diffuse reflectance, $\log(1/R)$. The diffuse reflectance was measured using a spectrophotometer V-670 with an integrating sphere unit ISN-723 (60-mm diameter, coated with barium sulphate). A pericarp disc with 20-mm diameter and 3-mm thickness was created using a punch and sandwiched by the two cover glasses and then attached to the light emitting window of the integrating sphere. The specular reflection was eliminated by tilting the window.

Table A1 Absorbance in the optical path (A), the ratio of absorbed photon number per incident photon number ($1-\exp(-A)$), fluorescence area (a.u. · nm), and fluorescence quantum yield (Φ). Excitation wavelength was 360 nm.

	A	$1-\exp(-A)$	Fluorescence area (a.u. · nm)	Φ
RhB	1.88×10^{-3} ± n.a.[†]	1.90×10^{-3} ± n.a.	6386 ± n.a.	0.69 – 0.97[§]
Tomato, day 1	2.02 ± 0.03[‡]	0.87 ± 0.00	9667 ± 319	2.3×10^{-3} – 3.2×10^{-3}[§]
day 13	1.98 ± 0.03[‡]	0.86 ± 0.00	16218 ± 371	3.8×10^{-3} – 5.4×10^{-3}[§]

[†] A of rhodamine B (RhB) was calculated from the absorption coefficient in the literature[9], the concentration in this experiment (0.094 μM) and the path length of the cell (10 mm).

[‡] A of tomato was calculated from the logarithmical value of diffuse reflectance R, $\log(1/R)$. R was measured using V-670 with INS-723 (JASCO Corp.).

[§] Φ of rhodamine B has uncertainty within the range, yielding the range for tomato samples as well. The errors were calculated using the error propagation's law from the standard error of three fruits.

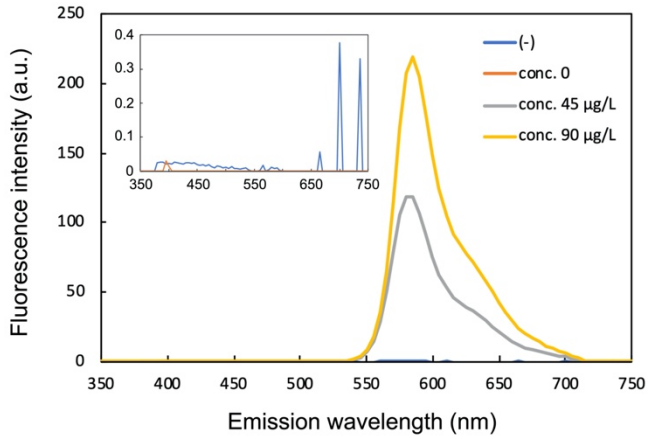

Fig. A1 Fluorescence emission spectra of rhodamine B in the same set-up. The data was obtained to calculate apparent fluorescence quantum yields of tomato surface tissues. (-) represents noise floor. The excitation wavelength was 360 nm.

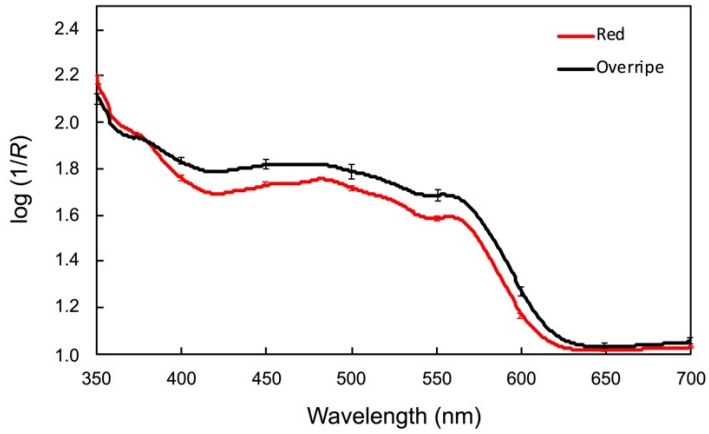

Fig. A2 Diffuse reflectance spectra of the tomato fruits. The red ripe and overripe fruits were destructively measured before and after the storage of 13 days. The error represents the standard error of three fruits.

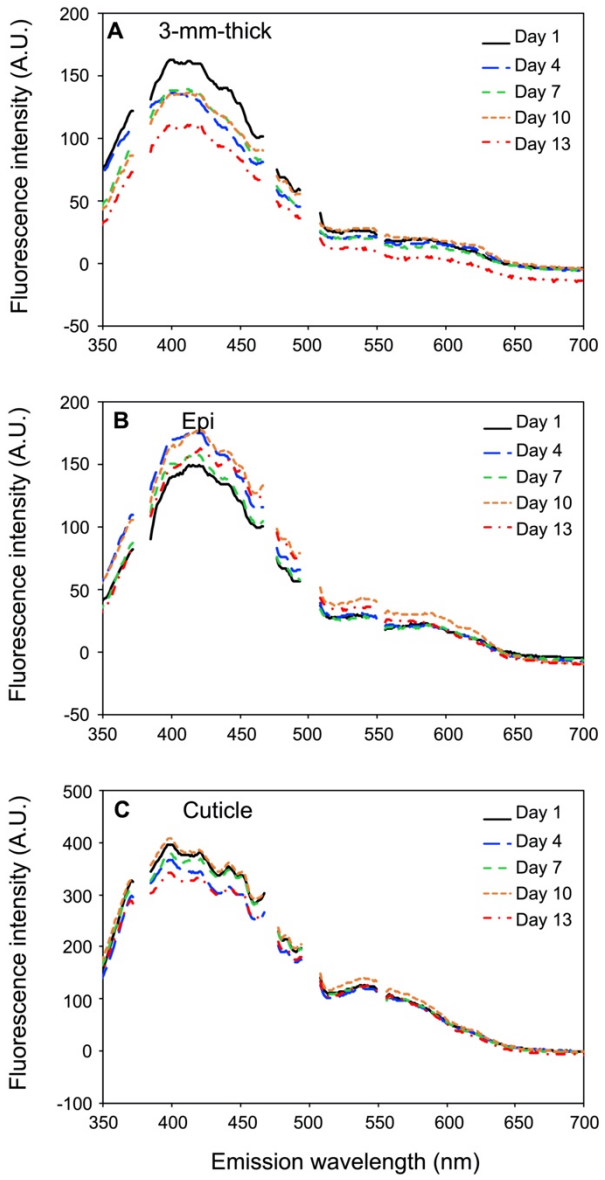

Fig. A3 Fluorescence emission spectra of (A) 3-mm-thick tomato sample, (B) epidermis (epi) and (C) cuticle during storage at 25 °C until day 13. The excitation wavelength was 250 nm. The standard error of three fruits ranged from 6 to 38 A.U. depending on the wavelength. Distortion from the changing filter at 370, 470 and 550 nm and the second order diffraction peak at 500 nm were removed.

References

1 USDA, United States Standards for Grades of Fresh Tomatoes. United States Department of Agriculture, Agricultural Marketing Service, Fruit and Vegetable Division, Fresh Products Branch, https://www.ams.usda.gov/sites/default/files/media/Tomato_Standard%5B1%5D.pdf, (accessed November 1, 2019).

2 T. Isaacson, D. K. Kosma, A. J. Matas, G. J. Buda, Y. He, B. Yu, A. Pravitasari, J. D. Batteas, R. E. Stark, M. A. Jenks and J. K. C. Rose, Cutin deficiency in the tomato fruit cuticle

consistently affects resistance to microbial infection and biomechanical properties, but not transpirational water loss, *The Plant Journal*, 2009, **60**, 363–377.

3 L. B. B. Martin and J. K. C. Rose, There's more than one way to skin a fruit: formation and functions of fruit cuticles, *Journal of Experimental Botany*, 2014, **65**, 4639–4651.

4 T. H. Yeats, G. J. Buda, Z. Wang, N. Chehanovsky, L. C. Moyle, R. Jetter, A. A. Schaffer and J. K. C. Rose, The fruit cuticles of wild tomato species exhibit architectural and chemical diversity, providing a new model for studying the evolution of cuticle function, *The Plant Journal*, 2012, **69**, 655–666.

5 J. Wu, M. S. Feld and R. P. Rava, Analytical model for extracting intrinsic fluorescence in turbid media, *Applied Optics*, 1993, **32**, 3585–3595.

6 D. Liu, X. Liu, Y. Zhang, Q. Wang and J. Lu, Tissue phantom-based breast cancer detection using continuous near-infrared sensor, *Bioengineered*, 2016, **7**, 321–326.

7 S. Pal, M. Mukherjee, B. Sen, S. Lohar and P. Chattopadhyay, Developement of a rhodamine-benzimidazol hybrid derivative as a novel FRET based chemosensor selective for trace level water, *RSC Advances*, 2014, **4**, 21608–21611.

8 C. Würth, M. Grabolle, J. Pauli, M. Spieles and U. Resch-Genger, Relative and absolute determination of fluorescence quantum yields of transparent samples, *Nature Protocols*, 2013, **8**, 1535–1550.

9 J. Muto, Optical properties of rhodamine B in the solutions of ethanol, acetic acid and water, *Keio engineering reports*, 1972, **25**, 71–84.